LABORATORY STUDIES IN UV AND EUV SOLAR PHYSICS

NASA Grant NAG5-9516

FINAL REPORT

For the period 1 June 2000 to 30 November 2004

Principal Investigator
Dr. John L. Kohl

March 2005

Prepared for
National Aeronautics and Space Administration
Washington, DC 20546

Smithsonian Institution
Astrophysical Observatory
60 Garden St.
Cambridge, MA   02138 U.S.A.

1.0 Introduction

A new 5 GHz Electron Cyclotron Resonance (ECR) ion source for SAO's Ion Beam Experiment was designed, built and tested. Absolute cross sections were measured for electron impact excitation (EIE) in C^{2+} ($2s2p\ ^3P^o - 2p^2\ ^3P$), and empirical EIE rate coefficients were derived. The absolute cross section for EIE in Si^{2+} ($3s3p\ ^3P^o - 3s3p\ ^1P^o$) was measured, and our experimental values for absolute cross sections for EIE in C^{3+} ($2s\ ^2S - 2p\ ^2P^o$) were reanalyzed and compared to values obtained by other experimental methods and by theory. In addition, a paper titled: "Electron Impact Excitation of $3s\ ^5S^o - 2s^2\ 2p^4\ ^3P$ Intercombination Lines and of Other Observationally Important Extreme-ultraviolet Lines in Ne^{2+}" was published.

The development and testing of the new ion source, the Si^{2+} EIE measurements, and the reevaluation of the cross sections for C^{3+} resulted from the Ph.D. research of Paul H. Janzen who completed the degree requirements for the Harvard University Department of Physics in 2002. John Kohl served as the Ph.D.Thesis Advisor.

Because of delays in bringing the new ion source on line, the measurements of EIE in C^{2+} ($2s2p\ ^3P^o - 2p^2\ ^3P$) were not completed until 2004. Preparations for measurements of EIE in C^{2+} ($1s^2\ ^1S - 2s2p\ ^1P^o$) are currently underway.

2.0 Development and Testing of the New 5GHz ECR Ion Source

The SAO 5 GHz ECR ion source was designed, built and tested by Paul Janzen as part of his Ph.D. thesis research. The essence of any ECR ion source is a magnetic field and microwave radiation with a relatively narrow frequency band. In any region of the source where the electron cyclotron frequency matches the microwave frequency, the electrons can be resonantly heated by the microwaves. If the electrons are sufficiently heated, ions will lose electrons through multiple electron impact ionization collisions that occur during the confinement time of the ion species of interest. Ions drift out of the source and are accelerated by an electric potential of 5 kV. The SAO 5 GHz ECR ion source has a conventional design, with permanent magnets, which supply a hexapole magnetic field, and electromagnets, which supply an axial magnetic field. Microwaves are supplied by a Varian 888-E klystron at up to 1.5 kW in the frequency range 4.4-5 GHz. The klystron locks to an input frequency provided by a 100 MHz quartz oscillator fed into a Miteq LP-4550 A that outputs 69 mW at the 48th harmonic of its input frequency. The exit aperture is made of Al with the side that faces the source, covered with a non-magnetic stainless steel plate. The ECR plasma forms inside a central tube. Wound around the tube are copper tubes through which cooling water flows. Each electromagnet is encased in a mild steel yoke; a 15 cm gap provides access for electrical current and for water cooling. The necessary power supplies and closed cycle water cooling and circulating systems were obtained. Some new lab infrastructure—additional electrical power and access to the building chilled-water system—was obtained. The necessary differential vacuum pumping systems and beam transport and species selection devices were already in place. Initial testing of the ion source used O_2 and Ar gas. The locations of the exit aperture and extraction electrodes were optimized using an iterative procedure. Source pressure,

microwave power, and the axial magnetic field were adjusted to optimize charge state output. Beam currents sufficient for EIE measurements of oxygen charge states up to 4+ and Ar charge states up to 5+ were obtained. CO_2 was introduced into the source and C^{2+} beams were extracted. A tuning procedure was used to steer the beam through the transport system and optimize its focus at the beams' intersection region. A beam current of about 120 nA was obtained.

3.0 Measurement of Electron Impact Excitation in C^{2+}

We have measured the absolute energy-averaged cross sections for EIE of the C^{2+} ($2s2p\ ^3P^o - 2p^2\ ^3P$) transition at energies from below threshold to 17 eV (see attached preprint). These cross sections cover a large enough energy range to determine the EIE rate coefficients for temperatures appropriate for astrophysical plasmas where C^{2+} is observed. The rate coefficients are needed for plasma diagnostic methods used to interpret the C III $\lambda117.6$ nm multiplet. Synchronous detection of decay photons was used together with a beams modulation technique and inclined electron and ion beams. Photons at $\lambda117.6$ nm from the decay of the excited ions were detected with an absolutely calibrated optical system. The fractional population of metastable C^{2+} ($2s2p\ ^3P^o$) in the incident ion beam was determined with a beam attenuation method using He gas. Forty two percent of the incident ions were found to be in the metastable state. The new SAO ECR ion source was used with CO_2 gas to produce the 120 nA C^{2+} incident beam current. The uncertainty in the empirical rate coefficient for 3.9×10^4 K was found to be $\pm14\%$ at 90% confidence (i.e. 1.65 σ). The measured cross section as a function of energy is in good agreement with 6-term close-coupling R-matrix calculations and 90-term R-matrix with pseudo-states calculations.

3.0 Measurement of Electron Impact Excitation in Si^{2+}

We have measured the absolute energy-averaged cross section for EIE of Si^{2+} ($3s3p\ ^3P^o - 3s3p\ ^1P^o$) from energies below threshold to the turn-on of the $3s3p\ ^3P^o - 3p^2\ ^3P$ transition. The synchronous photon detection technique with beams modulation and inclined electron and ion beams were used. Radiation at 120.65 nm from the decay of the excited ions to the $3s^2\ ^1S$ ground state was detected using an absolutely calibrated optical and detection system. The fractional population of metastable Si^{2+} ($3s3p\ ^3P^o$) in the incident ion beam was determined to be 0.256 ± 0.035 (1.65σ). Both the beam attenuation method and the intersystem decay photon method were used to determine the metastable state population fraction. The experimental energy spread ranged from 0.85 eV (FWHM) at the lowest energies to 0.56 eV at the highest. Resonance features consistent with 12-state close-coupling R-matrix calculations were distinguishable in the measured cross section.

4.0 Reevaluation of Electron Impact Excitation in C^{3+}

Experimental absolute rate coefficients for electron impact excitation of C^{3+} ($2s\ ^2S - 2p\ ^2P$) near threshold were measured by Daniel Savin as part of his Ph.D. thesis research.

They were reanalyzed to include a more accurate determination of the optical efficiency and revised radiometric uncertainties, which reduced the total systematic uncertainty of the results, but did not significantly change the measured value. Also, new R-matrix with pseudo states (RMPS) calculations for this transition near threshold were reported. Comparison of the RMPS results to those of simpler close-coupling calculations indicated the importance of accounting for target continuum effects. The reanalyzed results of Savin are in excellent agreement with the RMPS calculations. Comparisons were also made to other measurements of this excitation. Agreement with the RMPS results is better for the synchronous photon detection method used by the SAO group than for the results from the electron-energy loss method.

5.0 Publications and Presentations

The following publications and presentations resulted from the research carried out during the period of performance of the subject grant:

1. Absolute Cross Section for Electron Impact Excitation of Metastable C^{2+}, Adrian Daw, Larry Gardner, and John Kohl, 35th Meeting of the Division of Atomic, Molecular and Optical Physics, May 25-29, 2004, Tucson, AZ.
2. Measurement of the Absolute Electron Impact Excitation Cross Section for the C III 117.6 nm Transition, A. Daw, P. H. Janzen, L. D. Gardner, and J. L. Kohl, Bul. AAS 36, 801 (2004).
3. Advantages of the Photon Detection Method for Beams Measurements of Electron Impact Excitation Rates, J. L. Kohl, L.D. Gardner, and A. Daw, Bul. AAS 36, 753 (2004).
4. Absolute cross section for Si^{2+} ($3s3p\,^3P^o - 3s3p\,^1P^o$) Electron Impact Excitation, P. H. Janzen, L. D. Gardner, D. B. Reisenfeld, J. L. Kohl, Phys. Rev. A, 67, 052702, (2003).
5. Reevaluation of Experiments and New Theoretical Calculations for Electron Impact Excitation of C^{3+}, P. H. Janzen, L. D. Gardner, D. B. Reisenfeld, D. W. Savin, J. L. Kohl, Phys. Rev A, 59, 4821.
5. Electron Impact Excitation of 3s $^5S^o$-$2s^2\,2p^4\,^3P$ Intercombination Lines and of Other Observationally Important Extreme-Ultraviolet Lines in Ne III, B. M. McLaughlin, A. Daw, K. L. Bell, J. Phys. B, 35, 283 (2002).
6. An Experiment to Measure Electron Impact Excitation of Ions that have Metastable States, P. H. Janzen, Ph. D. Thesis, Harvard University, Department of Physics, (2002).
7. Absolute Cross Section for C^{2+} ($2s2p\,^3P^o - 2p^2\,^3P$) Electron Impact Excitation, A. Daw, L. D. Gardner, P. H. Janzen, J. L. Kohl, (see attached preprint).

Absolute cross section for $C^{2+}(2s2p\,^3P^\circ \to 2p^2\,^3P)$ electron impact excitation

A. Daw,* L. D. Gardner, P. H. Janzen,† and J. L. Kohl

Harvard-Smithsonian Center for Astrophysics, Cambridge, MA 02138

(Dated: March 30, 2005)

We have measured the absolute energy-averaged cross section for electron impact excitation (EIE) of $C^{2+}(2s2p\,^3P^\circ \to 2p^2\,^3P)$ from energies below threshold to 17 eV above, and present the measured absolute rate coefficients for this transition, for temperatures from 10^4 to 10^5 K. These rate coefficients are required for diagnostics of plasmas such as those found in astrophysical environments. The synchronous photon detection method with beams modulation and inclined electron and ion beams was used. Radiation at 117.6 nm from the decay of the excited ions back to the metastable state was detected using an absolutely calibrated optical system. The fractional population of metastable $C^{2+}(2s2p\,^3P^\circ)$ in the incident ion beam was determined to be $0.42 \pm 0.03(1.65\sigma)$. The rate coefficient for log T = 4.8 was determined to be $1.01 \times 10^{-8}\ cm^3 s^{-1} \pm 14\%$ at a 90% confidence (1.65σ) level. The measured cross section is in agreement within experimental uncertainty with 6-term close-coupling R-matrix calculations and 90-term R-matrix with psuedo-states calculations.

PACS numbers: 34.80.Kw, 34.80.Lx

I. INTRODUCTION

Electron-impact excitation (EIE) is the dominant mechanism for the formation of emission lines in many laboratory and astrophysical plasmas. Intensities of spectral lines arising from EIE can provide diagnostics of temperatures and densities of an emitting plasma, and of the abundance of elements in the plasma. Because the $C^{2+}(2s2p\,^3P^\circ \to 2p^2\,^3P)$ multiplet at λ 117.6 nm is excited by electron impact out of the metastable level, the ratio of the intensity of this emission to other emission lines of C^{2+} is a particularly valuable density diagnostic for solar plasmas [1–4], cataclysmic variable binary systems [5, 6], and cool stars in all stages of evolution [7–9].

Despite the fact that density diagnostics require accurate knowledge of the cross section for EIE out of metastable levels, few absolute measurements of such cross sections have been performed. Prior attempts are discussed by Janzen et al.,[10] who performed absolute measurements of the $Si^{2+}(3s3p\,^3P^\circ \to 3s3p\,^1P^\circ)$ EIE cross section using methods similar to those used in this work. Near-threshold measurements of the C^{2+} $(2s2p\,^3P^\circ \to 2p^2\,^3P)$ excitation have been performed by Bannister et al. [11] using the electron energy loss method and merged beams. There is a clear difference between the measured values of Bannister et al. and the theoretical calculations of Berrington et al.[12] for the C^{2+} $(2s2p\,^3P^\circ \to 2p^2\,^3P)$ excitation (Berrington, personal communication). The measurement reported here serves to investigate this discrepancy using a different experimental method that has an independent set of systematic uncertainties.

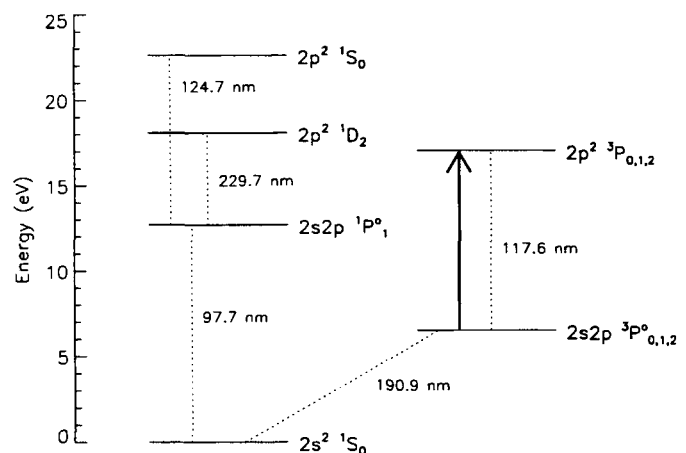Many of the relevant ions for astrophysics, particu-

FIG. 1: Partial term diagram for C^{2+}, showing astrophysically observed transitions. The arrow indicates the excitation under study.

larly ions used for density diagnostics, have EIE cross sections that are dominated by autoionizing resonances. Theoretical calculations for such ions are particularly difficult because the size of an individual resonance is extremely sensitive to the strength of the coupling to neighboring resonances [13]. When the R-matrix method of calculation was developed and applied to this problem, beryllium-like C^{2+} and O^{4+} were the first ions for which calculations were performed, owing to the astrophysical importance of these ions for density diagnostics and to the importance of resonances in the cross sections [12].

Using the unique capabilities of the synchronous photon detection method, the present work provides the first measurement of the EIE cross section for C^{2+} $(2s2p\,^3P^\circ \to 2p^2\,^3P)$ that covers the energy range required to determine rate coefficients for typical temperatures of formation of C^{2+} in astrophysical plasmas. (See Fig. 1.)

*Present address: Deptartment of Physics and Astronomy, Appalachian State University, Boone, NC 28608-2106
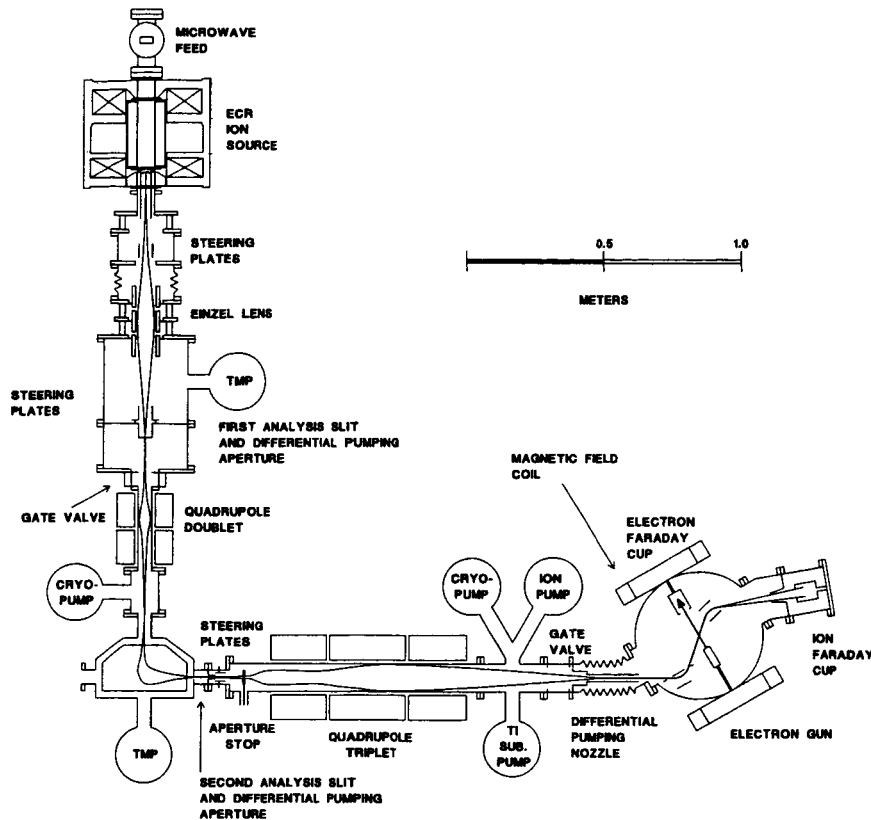†Present address: Los Alamos National Laboratory, MS D466, Los Alamos, NM 87545

FIG. 2: Overview of the experimental apparatus.

II. MEASUREMENTS

A. Apparatus and Technique

In the experiment EIE events were counted by detecting decay photons emitted from ions excited by electron impact. The basic apparatus is described by Janzen *et al.* [10] and by Reisenfeld *et al.* [14]. The principal modification to the apparatus since that work is the design and construction of a 4.8 GHz electron cyclotron resonance (ECR) ion source, which produces large currents of highly charged ions [15]. Ions are extracted at 5 kV, and charge to mass separated by a 90° deflection magnet to select C^{2+} ions. The beam of C^{2+} ions is then transported to the interaction chamber, sent through an electrostatic preanalyser, and crossed with an electron beam at 45° (see Fig. 2). An aperture stop in the beam transport system acts as a beam skimmer and serves to reduce the rate of background photons produced by collisions of ions with surfaces in the interaction chamber. Background photons produced by individual beams and the detector background were removed by using beams modulation whereby the beams were run individually and together in rapid succession. Typical ion current was 120 nA in the interaction chamber and typical electron current was 40 μA. A 15-22 G magnetic field is applied coaxially with the electron beam to collimate it and to increase its density. The distribution of current in both beams are measured with Faraday cups on an automated beams probe. Typical signal rates were 12 s^{-1} on a background of a few hundred per second. A large mirror subtending slightly over π steradians (sr) below the collision volume concentrates photons onto a KBr-coated microchannel plate detector (MCP), which itself subtends 0.32 sr (see Fig. 3). The KBr coating provided good detection efficiency at 117.6 nm. Calibrations of optical elements are performed separately and, together with a three-dimensional ray-tracing of the complete system, are used to determine the overall absolute photon detection efficiency. The absolute detected quantum efficiency of the MCP system was determined by referencing to a CsTe photodiode calibrated by the National Institute of Standards and Technology (NIST).

In the case where only one EIE transition contributes to the detected signal, which for this work applies to all collision energies below 16 eV, the EIE energy-averaged cross section is determined from the experimentally measured quantities via the equation

$$\langle \sigma \rangle \ = \ \frac{R_{sig}}{\xi \bar{v}_r} \ \frac{1}{\int N_I(\mathbf{x}) n_e(\mathbf{x}) \eta(\mathbf{x}, \tau) d^3\mathbf{x}}. \tag{1}$$

where R_{sig} is the EIE signal rate for the total solid angle collected by the experiment; ξ is the fraction of the
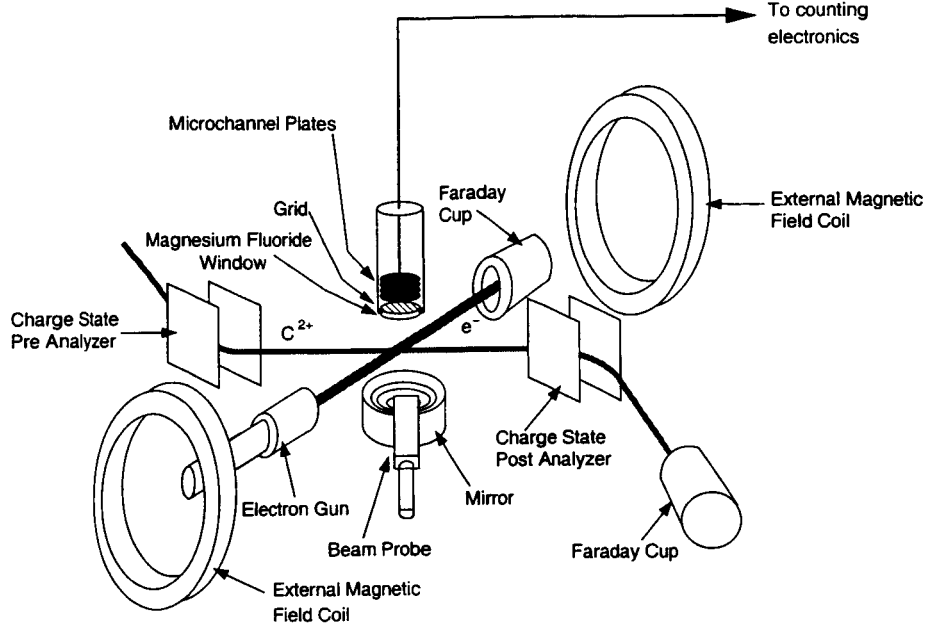
FIG. 3: Diagram of the interior of the interaction chamber.

TABLE I: Processes contributing to the measured signal.

Excitation Transition		Energy (eV)	λ (nm)	τ (ns)
$2s2p\,^3P^o$	$\longrightarrow 2p^2\,^3P$	10.55	117.6	0.75
	$\longrightarrow 2p^2\,^1S$	16.13	124.7	0.46
$2s^2\,^1S$	$\longrightarrow 2p^2\,^3P$	17.04	117.6	0.75
	$\longrightarrow 2p^2\,^1S$	22.63	124.7	0.46

ion beam in the initial state of the excitation process under study (see § II B); $\bar{v}_r$ is the average relative velocity; $N_I(\mathbf{x})$ and $n_e(\mathbf{x})$ are, respectively, the particle densities of the ion and electron beams at a location in the intersection volume denoted by the spatial coordinate $\mathbf{x}$; and $\eta(\mathbf{x}, \tau)$ is the spatially varying detection efficiency of the optical system where τ is the lifetime of the excited state. The dependence of $\eta(\mathbf{x}, \tau)$ on τ accounts for the fact that an ion excited at location $\mathbf{x}$ may radiate downstream of $\mathbf{x}$ because of the finite lifetime of the excited state. The lifetime of C^{2+} ($2p^2\,^3)P$ is 0.75 ns,[16, 17] which corresponds to a distance travelled of only 0.3 mm and a very minor effect on the detection efficiency η.

At collision energies above 16 eV, there is a small contribution (up to 5%) to the signal rate from other transitions, which produce light at wavelengths of 117.6 nm and 124.6 nm (see Fig. 1). To determine the $^3P^o \rightarrow {}^3P$ EIE cross section at the higher energies, these contributions are calculated and subtracted using the measured detection efficiencies, measured metastable fraction, and calculations of Mitnik et al. [18], as discussed in Section III. The absolute measured cross section is then integrated over Maxwellian velocity distributions to provide absolute measured rate coefficients for this astrophysically important transition.

B. Determination of the Metastable Fraction

The fraction of C^{2+} ions in the metastable $2s2p\,^3P^o$ state in the collision volume was determined by the beam attenuation method. Beam attenuation in fast ion beams is a well-established technique for determining the metastable fraction [19]. A single-species ion beam passing through a gas thickness $x = nL$, where n is the gas density and L is its length, will be attenuated by a factor $e^{-\sigma x}$, where σ is the attenuation coefficient, arising principally from electron capture. If the beam is composed of two components, ground-state ions and a fraction ξ of metastables, with attenuation cross sections σ and σ^* respectively, the current passing through will be

$$I(x) = I_0((1 - \xi)e^{-\sigma x} + \xi e^{-\sigma^* x}). \qquad (2)$$

The fraction of metastables can then be accurately determined, if σ and σ^* are sufficiently different, by measuring transmitted current as a function of pressure.

The region used for attenuation is between two differential pumping apertures which are roughly 1.5 m apart and located between the bending magnet and the interaction chamber (see Fig. 2). Pressure in the attenuation region varied with distance between the pumping apertures. The pressure was measured near the gas leak valve. Throughout the attenuation region, a magnetic quadrupole triplet lens focusses the C^{2+} beam through a differential pumping nozzle which leads to the interaction chamber. In the interaction chamber, the C^{2+} beam is electrostatically selected by a pre-analyzer and then again by a post-analyzer (see Fig. 3) before the remaining C^{2+} enters a Faraday cup.

A number of beam attenuation measurements were performed. Data collected using He as the attenuating
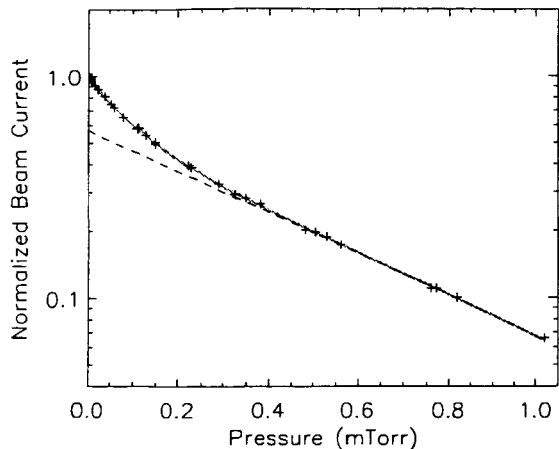
FIG. 4: Transmitted C^{2+} current vs He ion gauge pressure. The solid line is a two-exponential fit, and the dashed line indicates the current due to ground state ions.

gas are shown in Fig. 4. A two-exponential fit to the data, with constant fractional uncertainty in the current measurements, gives a ratio of $\sigma^*/\sigma = 5.1 \pm 0.3$ for the attenuation cross sections, and a fraction of $\xi = 0.424 \pm 0.015$ ions in the state with the higher attenuation cross section, where the listed 90% confidence (1.65σ) uncertainties arise from the fit covariance matrix. Because the electron capture cross section for C^{2+} in He is known to be significantly larger for the metastable state than for the ground state [20], we can identify $\xi = 0.424$ as the metastable fraction. However, uncertainty in the accuracy of pressure measurements, including up to 5% nonlinearity in the ionization gauge reading [21], increases the 90% uncertainty in ξ to 0.03.

The metastable fraction as determined by beam attenuation with He was corroborated by beam attenuation measurements with Ne, which indicated that $\sigma^*/\sigma = 0.64 \pm 0.03$ and that the metastable fraction was about 0.4. The electron capture cross section for C^{2+} in Ne is known to be $smaller$ for the metastable state than for the ground state [20].

During the $\sim 10\ \mu s$ transit time for C^{2+} ions from the ion source to the interaction chamber, radiative metastable decay is not a significant effect on the metastable fraction: of the three J levels in the $2s2p\ ^3P^\circ$ term, the $J = 1$ level, with its measured 9.714 ± 0.013 ms mean lifetime [22], decays considerably faster than the $J = 2$ and $J = 0$ levels. Even for the $J = 1$ level, the fraction of ions that will decay between the triplet, where the metastable fraction is measured, and the interaction region is only $\sim 0.03\%$, which is negligible.

The source was always operated in the same manner in order to ensure consistent results. The source generates its confinement field with a permanent magnet hexapole and electromagnet solenoids. The 4.8 GHz microwaves are supplied by a klystron, and CO_2 gas was used in the source for all C^{2+} data collection. A particular combination of source parameters maximized the C^{2+} current, and operating parameters were always set near the values that provided this maximum. The currents in the solenoids, for instance, were measured and maintained to an accuracy of 0.2%. Forward microwave power supplied to the source and reflected power from it, 400 W and 20 W respectively, were monitored and found to be consistent to 5%. The total output current of the source and the C^{2+} current in the interaction chamber were monitored and found to be stable and consistent for all data collection. Total output current was 0.27 mA within $\pm 6\%$.

Possible variation of the C^{2+} metastable fraction produced by the source was investigated by raising and lowering the source pressure to change total output current by +20% and -20%, respectively. The metastable fraction was measured under each of these operating conditions, which cover a wider range of conditions than those used for EIE data collection. Within the measurement uncertainty set by the linearity of the ionization gauge used for beam attenuation measurements, there was no significant effect on the metastable fraction. Similarly, for a range of microwave power wider than the range observed during EIE data collection, there was no significant effect on the source output.

C. Determination of the Photon Detection Efficiency

Optical system calibrations were performed at wavelengths of 116.5, 120, 121.6, 123.6, 130.5, and 189.8 nm by methods that are described in detail elsewhere [10, 14, 15]. The absolute detected counting efficiency of the MCP, reflectivity of the mirror, and transmittance of the MgF_2 window were measured. The angular and positional dependencies necessary for a full characterizaion of the system were also measured. The calibrations, together with a three-dimensional ray-tracing of the complete system, are used to determine the spatially varying photon detection efficiency. Interpolation between the calibration wavelengths of 116.5 and 120 nm determines the efficiency at 117.6 nm. As indicated by Table I, for incident electron energies above 16 eV, the possibility exists for other excitations that give rise to contributions to R_{sig} not only at 117.6 nm, but also at 124.7 nm. Since these contributions are small, the calibrations at 123.6 nm determine the detection efficiency at 124.7 nm to sufficient accuracy.

D. Uncertainties

Experimental uncertainties fall into two categories: statistical uncertainties which vary from point to point, and systematic uncertainties, which apply to all data points. The statistical uncertainties are reported at the
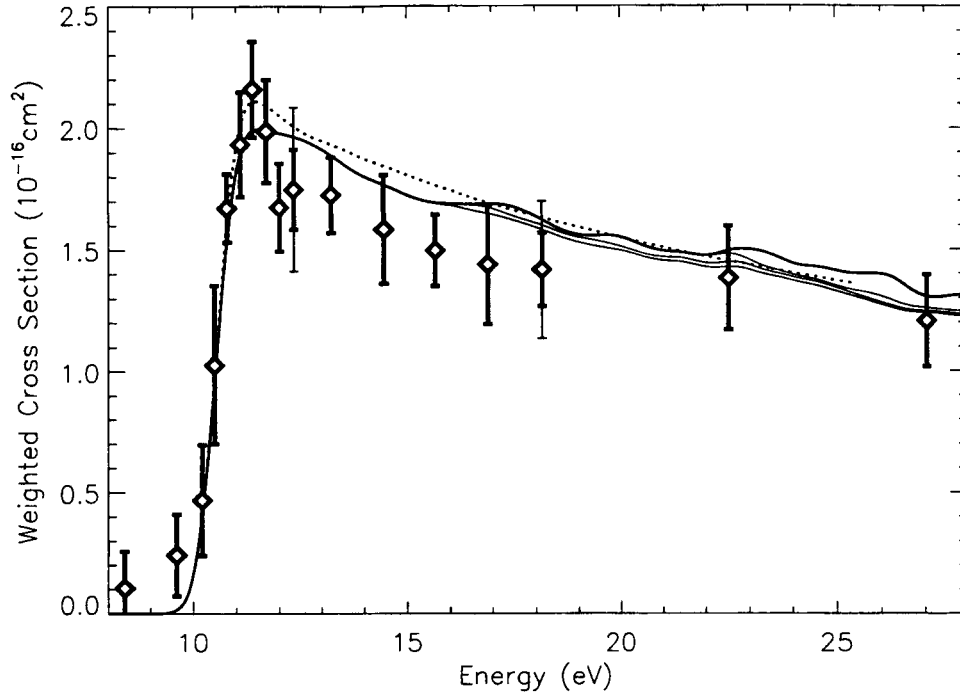
FIG. 5: Measured energy-averaged EIE cross section for the C^{2+} $(2s2p\ ^3P^\circ \to 2p^2\ ^3P)$ transition. The heavy error bars represent the statistical uncertainty at a 90% confidence level, and the thin error bars at 12.3 and 18.1 eV represent the total experimental uncertainty at a 90% confidence level. Above 16 eV the measured cross section includes small contributions from other states. The dotted curve shows the 6-term close-coupling R-matrix calculation of Berrington, et al. [12] and the solid curve shows the 90-term R-matrix with psuedostates calculation of Mitnik, et al. [18] Each has been convolved with the experimental energy spread of 0.9 eV (FWHM). The heavy solid curve shows the sum of the theoretical contributions of all transitions to the weighted cross section, incorporating the calculations of Mitnik et al., and the measured detection efficiencies and metastable fraction.

90% confidence limit (1.65σ). These uncertainties are typically $\sim$ 10% of the above-threshold cross section, with some points having statistical uncertainties as low as 8%.

The systematic uncertainty is 13% at 90% confidence. A summary of the known sources of systematic uncertainty for the present measurement, reported at the same (90%) confidence limit, is given in Table II. The dominant contributions are the uncertainty in the absolute efficiency of the NIST-calibrated photodiode used to determine the absolute efficiency of the MCP at 117.6 nm and the uncertainty in the metastable fraction. All uncertainties, systematic and statistical, were taken to be of random sign and uncorrelated, and were added in quadrature to determine the total experimental uncertainty.

III. RESULTS AND DISCUSSION

Our absolute measurement of the energy-averaged C^{2+} $(^3P^\circ \to\ ^3)P$ EIE cross section is presented in Fig. 5. The error bars on the data points represent total experimental uncertainty at a 90% confidence level. Also plot-

ted are the 6-term close-coupling R-matrix calculation of Berrington, et al. [11, 12] and the 90-term R-matrix with psuedostates calculation of Mitnik, et al. [18]. The calculation of Berrington et al. was shifted in energy so that the excitation threshold agrees with spectroscopic observations, while Mitnik et al. adjusted term energies to experimental values in their calculation process. Both calculations are convolved with the experimental energy distribution, which is represented as a 0.9-eV FWHM Gaussian.

Overall, both calculations are in good agreement with our experimental results, within experimental uncertainty and within the resolution allowed by the experimental energy spread.

Our cross section measurements are compared with those of Bannister et al. in Fig. 6. There are two curves shown for each calculation of the cross section, reflecting the two different experimental energy spreads. Bannister et al. used the electron energy loss/merged electron-ion beams technique, in which inelastically scattered electrons are deflected onto a position sensitive detector. With that method, a correction must be made for elastically scattered electrons that are also deflected onto the

TABLE II: Summary of systematic uncertainties. All uncertainties are quoted at a confidence level considered to be equivalent to a statistical 90% confidence level.

Sources of Uncertainty	Uncertainty
UNCERTAINTY IN BEAM DENSITIES	
Ion beam current measurement	3%
Electron beam current measurement	1%
Electron beam probe biasing procedure	5%
Uncertainty in metastable fraction	7%
UNCERTAINTIES IN BEAMS' GEOMETRIC OVERLAP	
Spatial coordinates of the collision volume	3%
Computational uncertainty in the overlap	1%
RADIOMETRIC CALIBRATION	
NIST standard photodiode accuracy	8%
Photodiode calibration variation	1%
MCP angular variation map	1%
Calibration of filters used in MCP calibration	2%
Variation in MCP QE	2%
Mirror reflectance	3%
MgF_2 window transmittance	3%
Computational error in raytracing program	1%
TOTAL QUARDATURE SUM	13%

FIG. 6: Absolute energy-averaged EIE cross section for the C^{2+} $(2s2p\ ^3P^\circ \rightarrow 2p^2\ ^3P)$ transition in the near-threshold region, comparing this measurement (black diamonds) to the measurement of Bannister et al. (grey squares). The error bars represent the statistical uncertainty at the 90% confidence level, and the thin error bars on every third data point represent the total experimental uncertainty. The black solid line and black dotted line show, respectively, the calculations of Berrington et al. [12] and Mitnik et al. [18] convolved with the 0.9 eV energy spread of this work. The grey solid and dotted lines show the the same calculations convolved with the 0.23 eV FWHM energy spread of the Bannister et al. experiment.

detector. This correction becomes more important for increasing energies above threshold, and the energy range of such experiments is limited to a few eV. A significant number of Bannister et al.'s error bars do not overlap the calculated cross sections. However, the metastable fraction was not measured directly and was instead assumed to be the same as that measured by Brazuk et al. ((0.56 ± 0.11 at a 1-σ confidence level) from a different ECR ion source running the same gas [23]. No uncertainty was attributed to this assumption or reflected in the reported absolute uncertainty of the cross sections.

Empirical rate coefficients for the C^{2+} $(2s2p\ ^3P^\circ \rightarrow 2p^2\ ^3)P$ transition are presented in Table III. These were determined by integrating the product of the measured cross section of this work and electron velocity in the ion rest frame over Maxwellian velocity distributions with temperatures from 10^4 to 10^5 K. The uncertainty in the rate coefficients due to the extrapolation is less than the statistical uncertainty of the measurements. The measured absolute cross section was corrected (5% or less) at energies above 16 eV to remove the contributions of other transitions. Also shown are the effective (i.e., thermally averaged) collision strengths as defined by Seaton [24], the statistical uncertainty in the integration at a 90% confidence level, and the fractional contribution to the rate coefficient from collision energies above 27 eV. This contribution, which is only significant at the higher temperatures, was determined by extrapolating from the measured cross sections using a simple power law. For any reasonable exponent in the power
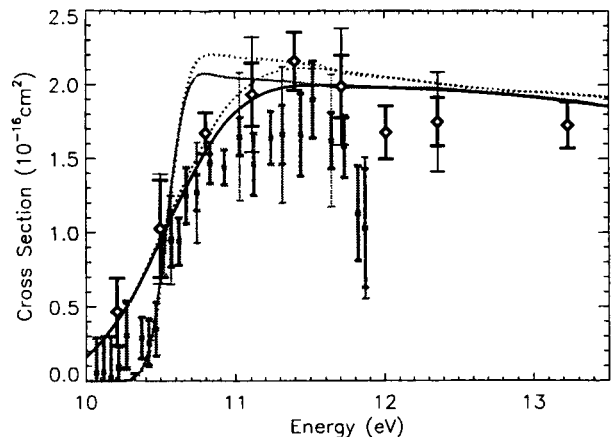
TABLE III: Measured rate coefficients, C, and effective collision strengths, Υ, for temperatures of interest, T, in astrophysics. The statistical uncertainty in C and Υ is presented in column 4. The quantity $f(E > 27$ eV) is the fraction of the rate coefficient that is determined by extrapolating to energies above the data point at 27 eV.

$Log_{10}(T)$	C (cm^{3}s^{-1})	Υ	% statistical uncertainty	$f(E > 27$ eV)
4.0	7.96e-13	17.2	5.8	0.000
4.2	5.77e-11	17.1	4.5	0.000
4.4	7.97e-10	17.2	3.8	0.001
4.6	3.90e-09	17.6	3.5	0.011
4.8	1.01e-08	18.4	3.6	0.065
5.0	1.75e-08	19.6	4.3	0.192

law, the effect on the rate coefficients was insignificant. The total 90% confidence uncertainty in the rate coefficients and effective collision strengths of 14% is given by the quadrature sum of the statistical uncertainty and the 13% systematic uncertainty in the overall scale of the cross section measurements.

IV. SUMMARY

We have determined the absolute cross section for electron impact excitation of $C^{2+}(2s2p\,^3P^\circ \rightarrow 2p^2\,^3P)$ for energies in the range 10 to 27 eV. The fraction of metastable $C^{2+}(2s2p\,^3P^\circ)$ in the beam was determined to be 0.42 ± 0.03 at 90% confidence. Empirical absolute rate coefficients for this transition are presented for temperatures from 10^4 to 10^5 K. Theory and experiment agree to within the experimental uncertainties.

Acknowledgments

[1] F. P. Keenan and G. A. Warren, Sol. Phys. **146**, 19 (1993).

[2] F. P. Keenan and K. A. Berrington, Sol. Phys. **99**, 25 (1985).

[3] F. Q. Orrall and E. J. Schmahl, Sol. Phys. **50**, 365 (1976).

[4] R. W. Noyes, J. C. Raymond, J. G. Doyle, and A. E. Kingston, Astrophys. J. **297**, 805 (1985).

[5] R. K. Prinja, K. S. Long, C. S. Froning, C. Knigge, D. K. Witherick, J. S. Clark, and F. A. Ringwald, Mon. Not. R. Astron. Soc. **340**, 551 (2003).

[6] R. K. Prinja, C. Knigge, D. K. Witherick, K. S. Long, and G. Brammer, Mon. Not. R. Astron. Soc. **355**, 137 (2004).

[7] E. F. Guinan, I. Ribas, and G. M. Harper, Astrophys. J. **594**, 561 (2003).

[8] E. Wilkinson, G. M. Harper, A. Brown, and G. J. Herczeg, Astron. J. **124**, 1077 (2002).

[9] C. Jordan, S. A. Sim, A. D. McMurry, and M. Aruvel, Mon. Not. R. Astron. Soc. **326**, 303 (2001).

[10] P. H. Janzen, L. D. Gardner, D. B. Reisenfeld, and J. L. Kohl, Phys. Rev. A **67**, 052702 (2003).

[11] M. E. Bannister, N. Djuric, O. Woitke, G. H. Dunn, Y. S. Chung, A. C. H. Smith, B. Wallbank, and K. A. Berrington, Int. J. Mass Spectrom. **192**, 39 (1999).

[12] K. A. Berrington, P. G. Burke, P. L. Dufton, and A. E. Kingston, J. Phys. B: Atom. Molec. Phys. **10**, 1465 (1977).

[13] D. C. Griffin, M. S. Pindzola, F. Robicheaux, T. W. Gorczyca, and N. R. Badnell, Phys. Rev. Lett. **72**, 3491 (1994).

[14] D. B. Reisenfeld, L. D. Gardner, P. H. Janzen, D. W. Savin, and J. L. Kohl, Phys. Rev. A **60**, 1153 (1999).

[15] P. H. Janzen, Ph. D. thesis, Harvard University (2002).

[16] C. Laughlin, E. R. Constantinides, and G. A. Victor, Journal of Physics B: Atom. Molec. Phys. **11**, 2243 (1978).

[17] Glass, R., J. Phys. B: Atom. Molec. Phys. **12**, 1633 (1979).

[18] D. M. Mitnik, D. C. Griffin, C. P. Ballance, and N. R. Badnell, J. Phys. B: Atom. Molec. Phys. **36**, 717 (2003).

[19] M. Vujovic, M. Matic, B. Cobic, and Y. Gordeev, J. Phys. B: Atom. Molec. Phys. **5**, 2085 (1972).

[20] M. Lennon, R. W. McCullough, and H. B. Gilbody, J. Phys. B: Atom. Molec. Phys. **16**, 2191 (1983).

[21] C. R. Tilford, J. Vac. Sci. Technol. **1**, 152 (1983).

[22] J. Doerfert, E. Träbert, A. Wolf, D. Schwalm, and O. Uwira, Phys. Rev. Lett. **78**, 4355 (1997).

[23] A. Brazuk, D. Dijkkamp, A. G. Drentje, F. J. de Heer, and H. Winter, Journal of Physics B: Atom. Molec. Phys. **17**, 2489 (1984).

[24] M. J. Seaton, Proc. Roy. Soc. A **218**, 400 (1953).